Am J Transl Res 2024;16(11):6867-6888
www.ajtr.org /ISSN:1943-8141/AJTR0159202

Original Article

Preliminary exploration of the role of CD14 mRNA in coronary artery injury in Kawasaki disease

Kun Zhu[1,2], Bo Wang[1], Huijuan Kan[3], Xiaoling Li[4], Xi Wang[4], Kangping Xu[4], Yu Pu[4], Zaidong Liu[4], Dongkai Wei[4], Wenhua Yan[1]

[1]Department of Cardiology, Children's Hospital of Soochow University, Suzhou, Jiangsu, China; [2]Department of Paediatrics, The First People's Hospital of Yan Cheng, Yancheng, Jiangsu, China; [3]Department of Paediatrics, The Affiliated Suzhou Hospital of Nanjing Medical University, Suzhou Municipal Hospital, Suzhou, Jiangsu, China; [4]Suzhou Func Biotech Inc., Suzhou, Jiangsu, China

Received July 15, 2024; Accepted October 24, 2024; Epub November 15, 2024; Published November 30, 2024

Abstract: Objective: Kawasaki disease (KD) is an acute vasculitis that typically occurs in young children and may lead to coronary artery lesions (CALs), but the precise mechanisms that trigger this illness are unclear. We hope to identify some clues to the pathogenesis of KD through clinical sample analysis. Methods: We included 12 children who had been diagnosed with KD coronary artery lesions (KD-CALs) or KD-no coronary artery lesions (KD-nCALs) and investigated the transcriptome variations of patients with KD in the acute and subacute stages. Further, we enrolled 12 new patients with KD and investigated the expression of CD14 mRNA and the downstream genes A20, A1/BF1_1, and IκBα, via real-time quantitative PCR (qRT-PCR). In addition, we established an animal model of KD-induced coronary inflammation and measured the protein levels of mCD14, IκBα and IL-6 on Day 7 and 14 after completion of modelling. Then, molecular docking was applied to analyse the binding power of the chemical compounds with mCD14. Results: The KD-CALs group contained 62 differentially expressed genes (DEGs), which were enriched in the nuclear factor kappa-B (NF-κB) signalling pathway. CD14 mRNA was upregulated in the acute stage, which caused an increase in expression of the downstream genes A20, A1/BF1_1, and IκBα. Molecular docking revealed that the best docking medicine with mCD14 was lupenone. On Day 14 after modelling, there was significant inflammation with infiltration of lymphocytes and macrophages in the coronary endothelium of the mice. Compared with those in the Day 7 group and the control group, the levels of mCD14, IκBα and IL-6 proteins in the coronary endothelium significantly increased in mice in the Day 14 group. Conclusions: CD14 mRNA may regulate IκBα expression and subsequently activate the NF-κB signalling pathway, ultimately causing vasculitis. CD14 mRNA participates in the occurrence of coronary artery injury, and its protein product mCD14 may be a potential therapeutic target for KD-CALs.

Keywords: CD14 mRNA, coronary artery lesions, Kawasaki disease, RNA-seq

Introduction

Kawasaki disease (KD), otherwise known as mucocutaneous lymph node syndrome, is an acute, self-limited systemic vasculitis in children. It affects small- and medium-sized blood vessels, and the main complication is coronary artery lesions [1, 2], including coronary artery dilation, aneurysm, and stenosis. Approximately 15%-25% of patients with KD develop CALs. The disease affects mostly children under five years of age, and in the industrialized world, it is the leading reason for acquired heart disease in children [3]. The incidence of KD differs across races and regions worldwide; in general, it is higher in Asia than in Europe and the United States. The epidemiology of KD among children under 5 years of age in East Asian countries such as Japan and South Korea shows that the incidence of KD has increased significantly in the past decade from 2009 to 2017. In China, the incidence has also shown an increasing trend in Beijing, Shanghai, Jiangsu, Guangdong, Hong Kong, Jilin and other regions [4]. The diagnosis of KD mainly depends on principal clinical features, including fever, rash, conjunctivitis,

https://doi.org/10.62347/GFSG6634

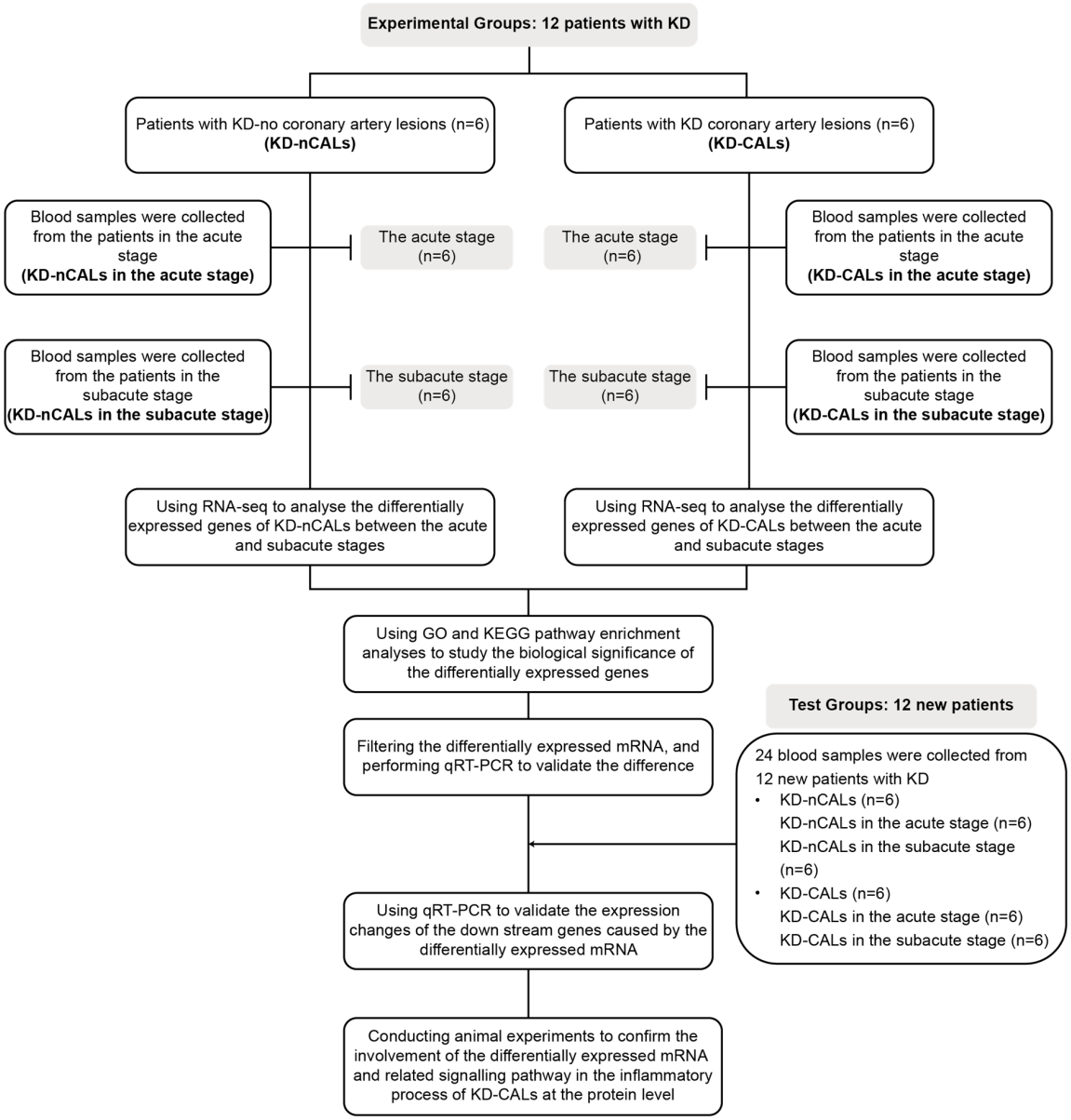

Figure 1. Flow chart of the research content. KD: Kawasaki disease; CALs: coronary artery lesions; nCALs: noncoronary artery lesions; GO: Gene Ontology; KEGG: Kyoto Encyclopaedia of Genes and Genomes; qRT-PCR: Real-time quantitative PCR.

lymphadenopathy, and changes in the oral mucosa and extremities [5]. Heart issues are more likely to occur in patients because of their unusual symptoms, which are frequently misdiagnosed and overlooked.

The cause of KD and the mechanisms underlying its development into CALs, however, are still unknown. It is generally believed that the aetiology of KD is an immune-mediated interaction between infection and genetic predisposition [6]. Other extrinsic factors, such as region, season, and climate, may also have an impact. Whole-genome association studies have identified several genes that are sensitive to KD, such as inositol-trisphosphate 3-kinase C (ITPKC), caspase 3 (CASP3), and cluster of differentiation 40 (CD40) [7]. Various pathogens, such as superantigen toxins, coronaviruses, and retroviruses, are considered triggering factors, but the exact pathogenic mechanism is not clear [8]. The activation of the immune sys-

Table 1. Classification of coronary artery abnormalities

Z value	Coronary artery abnormalities
< 2	No involvement
≥ 2- < 2.5	Dilation
≥ 2.5- < 5	Small coronary artery aneurysm
≥ 5- < 10	Medium coronary artery aneurysm
≥ 10	Enormous coronary artery aneurysm

tem provides crucial evidence for the pathophysiology of KD, and many inflammatory cytokines and cells, including tumour necrosis factor (TNF), interleukin (IL)-1β, interferon (IFN)-γ and peripheral lymphocytes, play a role in this process [9]. Some attempts have been made to identify clinical biomarkers of KD-CALs, such as sex, age, response to immunoglobulin, and red blood cell distribution width [10], but no additional studies on molecular biomarkers have been conducted.

Nuclear factor kappa-B (NF-κB) is widely present in animal cells and is a key regulatory gene in immunity and inflammation [11]. Previous studies have revealed that the activation of NF-κB can enhance the expression of various proinflammatory and proadhesion genes in vascular endothelial cells [12]. A study using mouse models of coronary atherosclerosis reported that vascular endothelial cells activated NF-κB signalling and upregulate the expression of NF-κB-induced genes, whereas the response of endothelial cells to specific inhibitor of NF-κB could depress the expression of relevant genes, thereby delaying the progression of arteriosclerosis [12]. The pathophysiology of intracranial aneurysms has been shown to be closely related to the NF-κB pathway, which affects smooth muscle cells and endothelial cells in blood vessels [13].

The CD14 protein was initially considered to be a membrane receptor (mCD14) for lipopolysaccharides on macrophages and to mediate the host response to sepsis. Additionally, mCD14 is also expressed in neutrophils and dendritic cells and with lower expression in human T cells, B cells, and intrinsic liver Kupffer cells [14]. It has also been detected in human intestinal cells, human and mouse liver cells, and pancreatic islets β cells. It participates in various pathological processes, such as immunity, infection, and cardiovascular disease [15], and is also closely related to KD. Geng et al. reported that the CD14+CD16- monocyte subsets related to neutrophil activation are significantly expanded in KD [16]. During 2019 coronavirus (COVID-19) infection, patients were reported to have severe vasculitis similar to KD. Liu et al. studied the possible mechanism responsible for the vascular injury in KD and COVID-19, and they found an increased proportion of CD14+ monocytes in patients with KD and COVID-19, which strengthened the adhesion and injury to vascular endothelial cells [17]. mCD14-related signalling pathways include NF-κB [18], and Aguilar Briseño et al. reported that in severe dengue fever virus (DENV) infection, mCD14 on blood monocytes was activated through the NF-κB pathway, ultimately driving the production of endothelial inflammation.

The traditional model in Western medicine development involves the identification of specific steps or highly specific inhibitors of protein targets during the disease process. However, most diseases, including cardiovascular and cerebrovascular diseases, comprise complex physiological and pathological processes involving the interaction of multiple genes and molecular networks, and therapeutic effects often cannot be achieved through the action of a single target. Traditional Chinese medicine (TCM) is natural and multitarget. Many studies have shown that TCM has therapeutic effects on inflammation, immunity, and cardiovascular and cerebrovascular diseases, including KD, through cytokines and signalling pathways [19, 20]. Tang et al. reported that some herbal chemicals which have effects on anti-inflammation or immunoregulation were considered as accessory treatment for patients with KD [21].

Our research aimed to explore the role of CD14 mRNA in coronary artery injury in patients with KD. **Figure 1** shows the study procedure. We examined the unique genes and signalling pathways involved in KD cases and found that CD14 mRNA might be involved in the signalling networks of KD-CALs, and thus, we detected the expression level of mCD14 in KD-CALs. Considering that it is difficult to obtain coronary tissue from patients with KD, we chose animal experiments for verification. We also attempted to determine whether mCD14 could serve as a therapeutic target for KD-CALs through molecular docking.

Table 2. Main experimental materials and chemicals

Materials and chemicals	Brand
CPT tubes	BD
Illumina TruSeq RNA Access kit	20020189, Illumina, USA
SuperScript® VILO™ cDNA Synthesis Kit	12594025, Invitrogen
TRIzol reagent	15596026, Invitrogen, Karlsruhe, Germany; Carlsbad, CA
Chloroform	288306, Sigma-Aldrich, St. Louis, MO, USA
Isopropanol	AC383910010, Fisher-Scientific, Thermo Fisher Scientific, Waltham, MA, USA
75% Ethanol	200-578-6, Sigma-Aldrich
Nuclease-free water	F0025, Solarbio
Environmentally friendly dewaxing solution	Solarbio YA0031
Anhydrous ethanol	Sangon A500737
Antigen repair solution	LEAGENE IH0297
Endogenous peroxidase blocker	Maixin Biological SP KIT-A3
Animal nonimmune serum	Maixin Biological SP KIT-B3
Secondary antibody +DAB reagent kit	DAKO K5007
Haematoxylin	Sangon E607307-100
Eosin staining solution	Sangon E607317-100
Microscope	Nikon ECLIPSE CI-L
$(NH_4)_2SO_4$	Sangon
$CuSO_4$ $5H_2O$	Sangon
$FeSO_4$ $7H_2O$	Sangon
$MgSO_4$ $7H_2O$	Sangon
$CaCl_2$ $2H_2O$	Sangon
$ZnSO_4$ $7H_2O$	Sangon
KH_2PO_4	Sangon
Biotin	Sangon
Sucrose	Biosharp
Acetone	Sinopharm 10000418
YM broth culture medium powder	Sangon
1× PBS Buffer	Servicebio

Materials and methods

Clinical experiments

Patients in the KD group: Patient inclusion criteria: 1. Meeting the 2017 edition of the Diagnosis, Treatment, and Long-term Management of Kawasaki Disease - Scientific Statement of the American Heart Association for Medical Professionals [22], with fever lasting for more than 5 days (including those with fever < 5 days after treatment); bilateral conjunctival congestion; oral manifestations: redness of the lips, strawberry tongue, diffuse congestion of the oral mucosa; irregular rash; extremity changes: swelling of the hands and feet in the acute stage, finger and toe peeling during the recovery period; and nonpurulent cervical lymphadenopathy during the acute phase. The presence of 5 of the above 6 main symptoms can indicate a diagnosis of KD. In the event that only 4 of the above 6 symptoms are present, but coronary artery aneurysm (or dilation) was confirmed through echocardiography or angiocardiography, and other diseases could be ruled out, a diagnosis of KD was confirmed. 2. Parents agreed to undergo blood tests in the acute and subacute stages during hospitalization at Soochow University Affiliated Children's Hospital, and we obtained a signed informed consent form from the legal guardian of each patient. The case exclusion criteria were children who were not diagnosed with KD upon discharge and were unable to complete blood tests for various reasons.

Finally, 24 patients who were diagnosed with KD for the first time in the Cardiology Department of Soochow University Affiliated Children's Hospital (Suzhou, Jiangsu Province,

Table 3. Primer sequences for RNA

Gene name	Sequence (5'-3')	Product length (bp)	Tm	GC%	Reference Sequence
CD14	CTGCAACTTCTCCGAACCTC	215	58.57	55	NM_000591.4
	CCAGTAGCTGAGCAGGAACC		60.11	60	
A20	ATGCACCGATACACACTGGA	153	59.1	50	NM_001270507.2
	CACAAGCTTCCGGACTTCTC		58.57	55	
A1/Bf1_1	TTACAGGCTGGCTCAGGACT	87	60.55	55	NM_001114735.2
	AGCACTCTGGACGTTTTGCT		60.18	50	
IκBα	GCTGATGTCAATGCTCAGGA	103	57.97	50	NM_020529.3
	CCCCACACTTCAACAGGAGT		59.53	55	

China) were enrolled from June 2021 to March 2022. According to the 2017 edition of *Diagnosis, Treatment, and Long-term Management of Kawasaki Disease - American Heart Association's Scientific Statement to Medical Professionals* [22], the standard for determining whether patients with KD have concomitant coronary artery damage is the *Z* value, which is the coronary artery diameter corrected by body surface area, rather than only the absolute value of diameter. The classification of coronary artery abnormalities is based on the *Z* value (**Table 1**). We performed echocardiography on the second day after admission and 3 days after reaching normal body temperature and selected patients with a *Z*-value greater than 2 as the CALs. Patients with KD were subsequently divided into the CALs and non-CALs (nCLAs) groups, which consisted of 12 patients each. Each group was subdivided into the acute phase (before intravenous immunoglobulin infusion, 1-10 days after onset) and the subacute phase (after intravenous immunoglobulin infusion, body temperature returned to normal, 11-21 days after onset). Clinical data, including age, sex, weight, duration of fever, clinical manifestations, and response to immunoglobulin therapy, were collected for the two groups.

Isolation of peripheral blood mononuclear cells: The peripheral blood samples in each group were collected in the acute and subacute stages, with 2 millilitres of blood drawn from each patient into an EDTA anticoagulant tube. Peripheral blood mononuclear cells (PBMCs) were isolated from blood donors using CPT tubes. Isolated PBMCs were lysed in TRIzol reagent (1 ml/1×10^7 PBMCs) and stored at -80°C until further processing.

Total RNA extraction: The PBMCs immersed in TRIzol were removed from -80°C and thawed on ice, mixed by whirling for 1 min and left at room temperature for 5 min. Chloroform was added to purify the samples, followed by vortexing, incubation for 5 min at room temperature, and centrifugation for 15 min (12,000× g, 4°C). The aqueous phase containing the RNA was transferred to a new tube, followed by the addition of isopropanol, and the samples were centrifuged for 15 min (12,000× g, 4°C) and then incubated at room temperature for 10 min. The RNA was washed with 75% ethanol, air-dried, and resuspended in 50 μl of nuclease-free water. The brand and catalogue for all the materials and chemicals used in this study are listed in **Table 2**.

mRNA library construction and sequencing: Total RNA sequencing libraries were constructed using the Illumina TruSeq RNA Access Kit. Sequencing procedures were performed on an Illumina NovaSeq 6000 platform with 150-bp paired-end reads at an average depth of 75 million reads. RNA libraries were constructed and sequenced. The expression level was quantified by the count per million method, and the relative expression level was expressed as the log2 of the fold change (FC). A log2FC greater than 1 (|Log2FC| > 1) was considered high, and a log2FC less than -1 (|Log2FC| < -1) was considered low.

Reverse transcription and real-time quantitative PCR: Total RNA was extracted from the PBMCs following the steps described in "Total RNA Extraction". A nucleic acid quantification detector was used to measure the RNA concentration. cDNA was synthesized using the SuperScript® VILO™ cDNA Synthesis Kit, and the cDNA was subsequently used as a template to amplify the extracted RNA via the PCR instrument for reverse transcription. Real-time quantitative PCR (qRT-PCR) was performed using the SYBR Green dye method. The total

Table 4. 4 L of C-limiting culture medium

$(NH_4)_2SO_4$	8 g
KH_2PO_4	8 g
$MgSO_4$ $7H_2O$	0.2 g
$CaCl_2$ $2H_2O$	0.2 g
$CuSO_4$ $5H_2O$	0.004 g
$FeSO_4$ $7H_2O$	0.04 g
$ZnSO_4$ $7H_2O$	0.004 g
Sucrose	200 g
Biotin	100 μl

The pH was adjusted to 5.2, and pure water was added to bring the volume to 4 L.

RNA qPCR primers were designed on the basis of RNA sequences from NCBI (the sequences of the primers used for RNA are listed in **Table 3**). These reactions were all performed in duplicate in 96-well plates, and the data were evaluated using a 7900HT Fast Real-Time PCR system.

Analyses of differentially expressed genes (DEGs) and functional enrichment: The edge R algorithm was applied to identify the DEGs between the acute and subacute stages in each group. Genes with a |log2FC| > 1.0 and a false discovery rate value < 0.05 were defined as DEGs. In addition, Gene Ontology (GO) and Kyoto Encyclopaedia of Genes and Genomes (KEGG) functional enrichment analyses were utilized to explore the signalling pathways and biological processes associated with the enriched DEGs.

Construction of the protein interaction network: We searched the STRING database (https://string-db.org/) using a single protein name ("CD14") and organism (*"Homo sapiens"*). Subsequently, we set the following parameters to characterize the interaction network and obtain the top 50 key proteins related to CD14: minimum required score ["highest confidence (0.900)"], the meaning of network edges ("evidence"), the maximum number of interactors to show ("no more than 50 interactors" in the 1st shell) and active interaction sources ("Text mining", "Experiments", "Databases", "Coexpression").

Molecular docking simulation: The process of molecular docking translation, including the specific software utilized and their corresponding parameters, was delineated as follows:

Protein structure acquisition: The 3D protein structure of mCD14 was downloaded from the RCSB Protein Data Bank (RCSB PDB) (http://www.rcsb.org/).

Protein structure refinement: The protein structure, once acquired, was preprocessed using AutoDock Tools 1.5.6. In this phase, the parameters were set to exclusively utilize polar entities, incorporate polar hydrogen, calculate charges using the Gasteiger method, and preserve water molecules.

Acquisition of drug molecules: A total of 104 variants of natural product molecules derived from traditional Chinese medicine were procured in MOL2 format from the TCM Database of Taiwan. These molecules were subsequently transformed into PDB format using Open Babel.

Preprocessing of drug molecules: Subsequently, the drug molecules were transformed from PDB format to PDBQT format using MGL Tools, specifically for molecular docking. During this phase, it was necessary to retain H atoms and incorporate the -F parameter, among other requirements.

Molecular docking: In the final stage, these small molecules were docked onto the protein via AutoDock Vina. The energy range was set to 2 kcal/mol, and the number of modes was set to 9.

Analysis of results: The docking results were subsequently visualized and scrutinized using PyMol. The binding modes of the drug molecules on the protein were observed, and the binding energy was computed.

Animal experiments

Animals: For the experiments, 4-week-old C57BL/6J male mice with a body weight of 16±1.8 g were purchased from Hangzhou Ziyuan Experimental Animal Technology Co., Ltd. (SCXK Zhejiang 2019-0004). The animals had cages with multilayer laminar air flow in the Animal Experimental Center of Suzhou University Affiliated Children's Hospital, with 12 hours of light and dark. The temperature of the animal room was controlled at 24±2°C, the relative humidity was maintained at 55±5%, and the noise was less than 50 decibels. With fewer than 5 mice per cage and provision of

Table 5. General characteristics of the KD patients in the two groups

	nCALs (n = 12)	CALs (n = 12)	*Z/t*	*P*
Gender			/	1.000
Male	9 (75.0%)	10 (83.3%)		
Female	3 (25.0%)	2 (16.7%)		
Age (M)	38.00 (28.50-72.25)	24.00 (15.50-28.50)	-2.430[b]	0.015*
Weight (kg)	16.00 (14.25-19.75)	12.75 (12.00-14.75)	-2.405[b]	0.016*
Duration of fever(D)	5.21±0.89	5.33±0.98	-0.326[a]	0.747
IVIG response			/	0.640
-	2 (16.7%)	4 (33.3%)		
+	10 (83.3%)	8 (66.7%)		

a: *t* value; b: *Z* value; *: P < 0.05 statistically significant. A normality test was conducted using the Shapiro-Wilk test, and the duration of fever was normally distributed and expressed as the mean ± standard deviation ($\bar{x}$ ±s). An independent sample t test was used for intergroup comparisons. Age and nonnormally distributed weight data are expressed as the median and interquartile range M (P25, P75), and the Mann-Whitney U test was used for intergroup comparisons. Gender and immunoglobulin (IVIG) response as count data are expressed as percentages (%), and Fisher's exact probability method was used for intergroup comparisons.

Table 6. Clinical manifestations of KD patients in the two groups

	nCALs (n = 12)	CALs (n = 12)	C^2	*P*
Rash (+/-)	7/5	6/6	/	1.000
Conjunctivitis (+/-)	10/2	9/3	/	1.000
Oral changes (+/-)	10/2	9/3	/	1.000
Strawberry tongue (+/-)	9/3	8/4	/	1.000
Cervical lymphadenopathy (+/-)	9/3	8/4	/	1.000
Extremity changes (+/-)	7/5	8/4	/	1.000
BCG scar (+/-)	3/9	5/7	/	0.667
Peeling (+/-)	8/4	7/5	/	1.000

P < 0.05 indicated statistical significance. Count data are expressed as percentages (%), and Fisher's exact probability method was used for intergroup comparisons.

purified drinking water and standard feed, this experiment strictly followed the requirements of the Regulations on the Management of Experimental Animals issued by the Ministry of Science and Technology of the People's Republic of China. Approval from the Ethics Committee of Experimental Animals at Suzhou University was obtained, and relevant experiments were conducted in accordance with the "3R" principle.

Preparation of Candida albicans water solution (CAWS): The *Candida albicans* strain used in this experiment was NBRC 1385, which was purchased from the China Industrial Microbial Strain Collection and Management Center in Osaka, Japan.

(1) A total of 8.4 of YM broth culture medium powder was added, followed by 400 ml pure and sterilization under high pressure at 115°C for 20 minutes; (2) The YM broth culture obtained from the first step, followed by the addition of 4 ml of preserved white yeast, mixing well, and shaking on a shaker for 48-72 hours (27°C, 200 rpm); (3) A total of 4 L of C-containing culture medium was prepared (**Table 4**), divided into 8 conical flasks of 500 ml/bottle, and sterilized under high pressure at 115°C for 20 minutes. After cooling, the bacterial mixture shaken in step 2 was evenly distributed into each conical flask and shaken for 48 hours (27°C, 200 rpm); (4) After shaking for 48 hours, an equal amount of anhydrous ethanol was added to each conical flask, which was subsequently stored overnight at 4°C; (5) The overnight mixture was poured into a 50-ml centrifuge tube, and centrifuged at 4°C at 9000 rpm for 15 minutes, then, the supernatant was discarded. The precipitate was dissolved in water by vortexing and poured into a

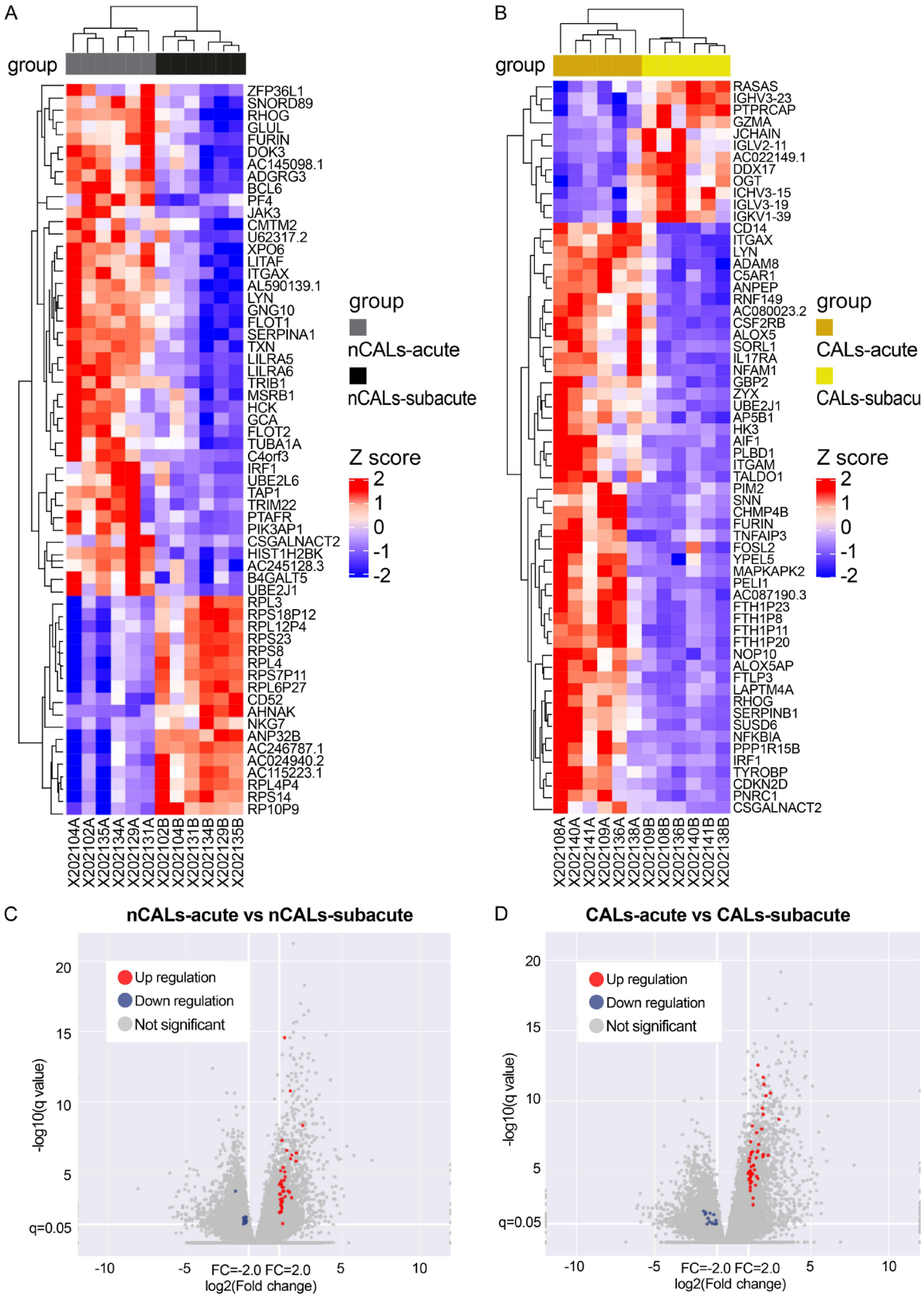

Figure 2. Heatmap (A, B) and volcano map (C, D) of the differential mRNA expression of KD in the acute and subacute stages with and without CALs. (A) Heatmap of 60 genes differentially expressed in children without coronary dilatation in the acute stage compared with those in the subacute stage. (B) Heatmap of 62 genes differentially

expressed in children with coronary dilatation in the acute stage compared with those in the subacute stage. (C) Volcano plot of expressed mRNAs in the KD-nCALs group. (D) Volcano plot of expressed mRNAs in the KD-CALs group. KD: Kawasaki disease; CALs: coronary artery lesions.

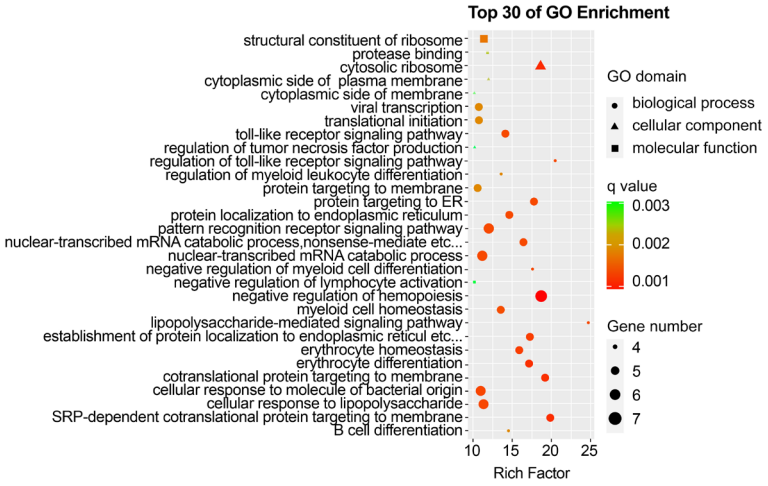

Figure 3. Top 30 enriched GO terms in the KD-nCALs group. GO: Gene Ontology; KD: Kawasaki disease; CALs: coronary artery lesions.

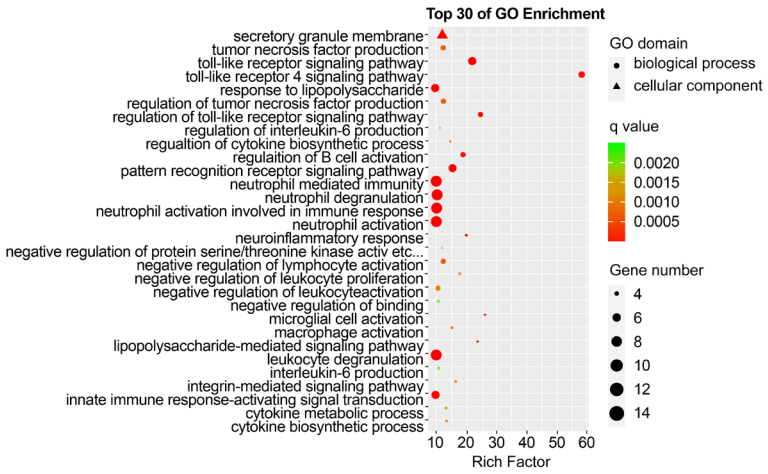

Figure 4. Top 30 enriched GO terms in the KD-CALs group. GO: Gene Ontology; KD: Kawasaki disease; CALs: coronary artery lesions.

measuring cup. Thereafter, 500 ml water was added in the cup, and subsequently dissolved in a rotor for 2 hours. The precipitate was divided into a 50-ml centrifuge tube and then centrifuged at 4°C at 9000 rpm for 15 minutes. The supernatant was poured into a clean beaker, followed by the addition of an equal amount of anhydrous ethanol and storage overnight at 4°C; (6) After overnight incubation, the solution was mixed by rotating with a pipette and then centrifuged at 9000 rpm for 15 minutes at 4°C. After the supernatant was discarded, the precipitate was dissolved in a small amount of acetone (20-30 ml), and the mixture was centrifuged in a 50-ml centrifuge tube at 3000 rpm for 10 minutes at 4°C. Then, the supernatant was discarded with a pipette, and the precipitate was allowed to air dry in a fume hood for at least 3 days; (7) After air drying, the dried material was weighed and divided into 20 mg samples per tube, and 1 ml of 1× PBS was added to each tube to dissolve. The samples were then stored at -80°C for later use.

Preparation of a mouse model of KD coronary inflammation: Construction of the mouse KD-CALs model was carried out via the intraperitoneal injection of CAWS. The prepared 20 mg/ml CAWS was injected intraperitoneally into each mouse, with 4 mg of CAWS or 0.2 ml once a day at the same time in the morning for 5 consecutive days. After the injection, tissues were collected at different time points, including Days 7 and 14 after the injection was completed.

Animal experimental grouping: The mice were randomly divided into a control group and a model group. The control group included 3 mice that received 0.2 ml of 1× PBS at the same time every morning. The model group was subdivided into a Day 7 group and a Day 14 group based on the sampling time after injection, each of which included 4 mice.

Processing of animal vascular samples: At 8:00 am on the 7th and 14th days after injection, after being anesthetized by an appropriate inhalation of isoflurane, four mice each time

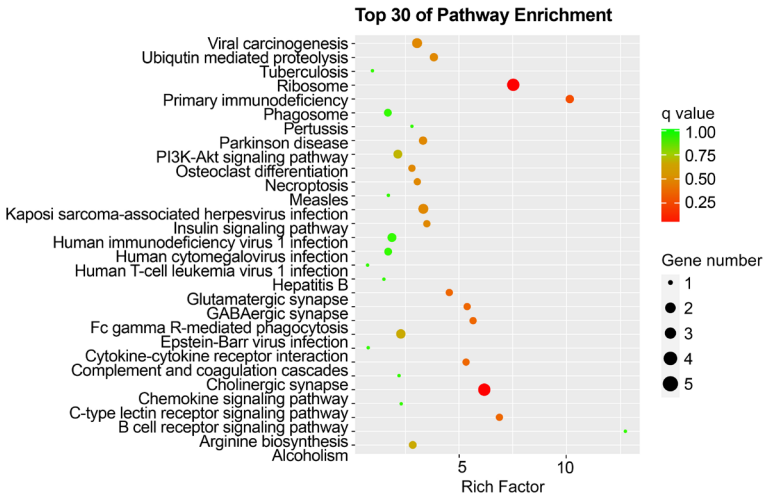

Figure 5. Top 30 enriched pathways in the KD-nCALs group. KD: Kawasaki disease; CALs: coronary artery lesions.

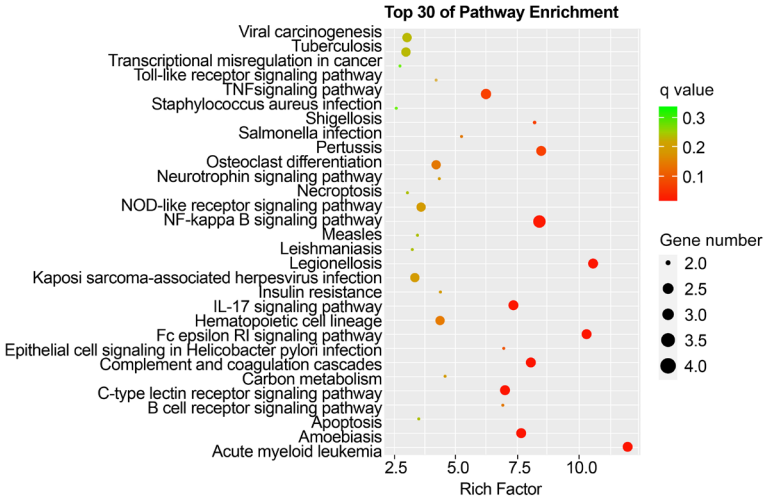

Figure 6. Top 30 enriched pathways in the KD-CALs group. KD: Kawasaki disease; CALs: coronary artery lesions.

were euthanized via the cervical dislocation method, and the coronary artery specimens were separated and collected under a microscope. Inflammation was observed via H&E staining of case sections, and detection of mCD14, IκBα and IL-6 proteins in coronary artery specimens was performed via immunohistochemistry.

Immunohistochemistry: (1) The baked tissue was sliced at 60-65°C for 2 hours and then soaked twice in environmentally friendly dewaxing solution for 15 minutes each time. The samples were then immersed twice in 100% ethanol for 5 minutes each time, followed by 95% and 75% ethanol sequentially for 5 minutes each time. After dewaxing, the samples were rinsed with purified water 1-2 times and then placed in pure water until the antigen repair stage. (2) Two tissue slices were immersed in diluted antigen repair solution, the power of the induction cooker was set to 800-1200 W, and the pressure valve of the pressure cooker was set to start spraying for 3 minutes. After 5 minutes, the power was turned off, the pressure cooker was exhausted, the sections were removed, and the samples were cooled naturally at room temperature. The repair solution was discarded, the samples were rinsed with purified water three times, and an immunohistochemical oil pen was used to circle around the tissue. (3) Three drops of endogenous peroxidase blocker were added to completely cover the tissue, which was subsequently incubated at room temperature for 10 minutes. The samples were rinsed with 1× PBS cleaning buffer three times. (4) Four drops of goat serum blocking solution were added to completely cover the tissue, which was subsequently incubated at room temperature for 15 minutes, after which the blocking solution was removed by shaking. (5) The antibody was diluted in proportion to the antibody mixture, and the diluted antibody was added to completely cover the tissue. The samples were incubated overnight at 4°C and rinsed with 1× PBS three times for 5 minutes each. (6) HRP-labelled secondary antibodies corresponding to the primary antibodies were added, and the samples were incubated at room temperature for 30 minutes. The samples were rinsed 3 times with 1× PBS for 5 minutes each. (7) The DAB colour solution was prepared at a 1:50 ratio to incubate the samples at room temperature for 3 minutes, and colour development was stopped

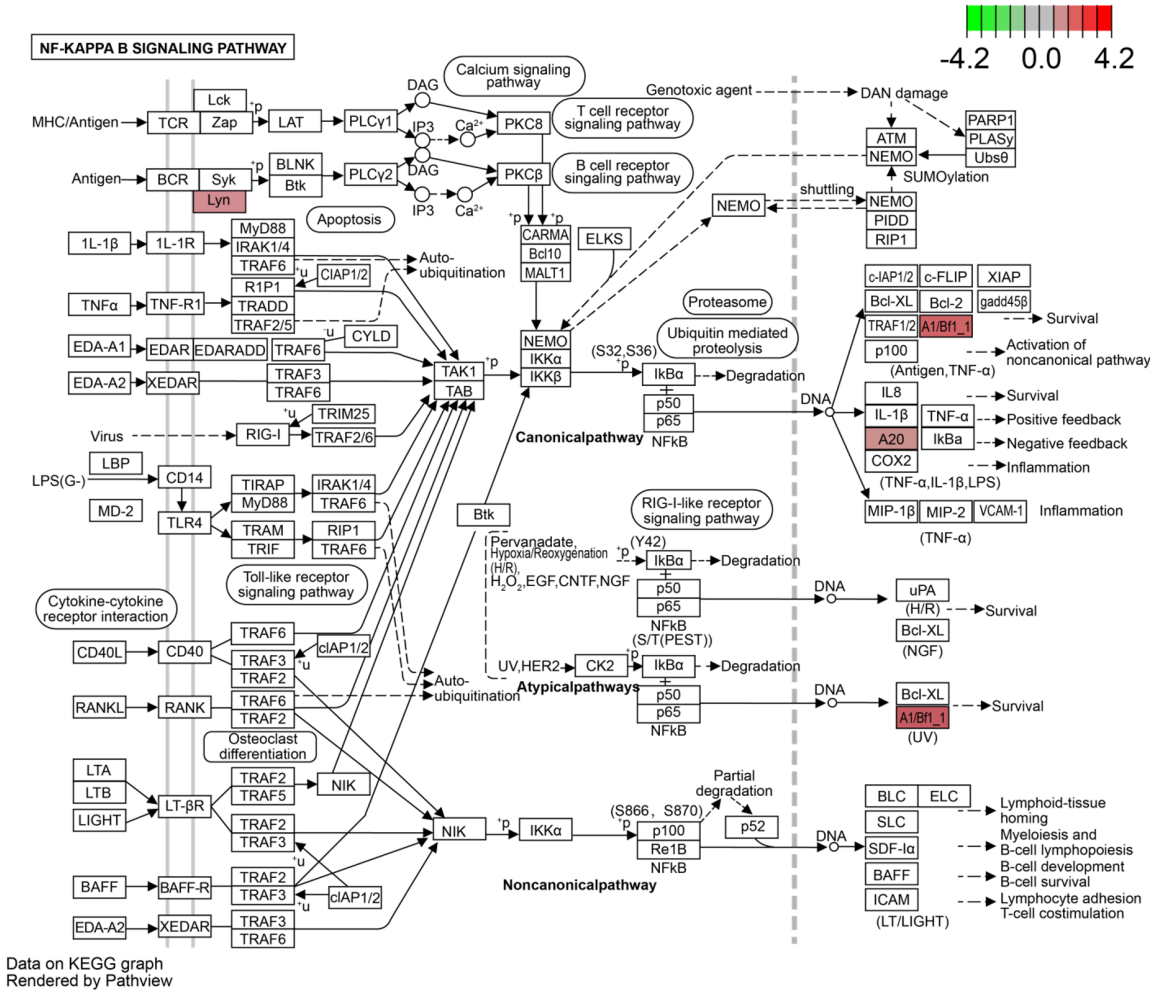

Figure 7. NF-κB signalling pathway in the KD-nCALs group. KD: Kawasaki disease; CALs: coronary artery lesions.

with tap water. Haematoxylin-stained sections were restained for 2 minutes, washed 2-3 times with tap water, soaked in hydrochloric acid alcohol differentiation solution for 30 seconds, washed 2-3 times with tap water, and returned to blue in tap water for 2-3 minutes. The samples were soaked in 75% and 95% ethanol for 1 min each time and then soaked twice in 100% ethanol for 5 min each time. (8) The samples were sealed with neutral gum, air dried naturally, and scanned with a panoramic scanner.

Pathological sections: (1) Sample collection and dehydration. (2) After being embedded in paraffin, the samples were cut to a thickness of 3 μm. (3) The sections were then incubated in an oven at 60°C for 30 minutes. (4) The samples were subjected to environmentally friendly dewaxing solution I for 10 minutes, environmentally friendly dewaxing solution II for 5 minutes, environmentally friendly dewaxing solution III for 5 minutes, anhydrous ethanol for 5 minutes, anhydrous ethanol for 2 minutes, 95% alcohol for 2 minutes, 80% alcohol for 2 minutes, water washing for 2 minutes, haematoxylin staining solution for 1-5 minutes, water washing for 5 minutes, rapid differentiation of the differentiation solution, warm water washing for returning blue, eosin staining solution for 5 minutes, 95% alcohol for 1-2 minutes, anhydrous ethanol for 1-3 minutes, anhydrous ethanol for 1-3 minutes, and environmentally friendly dewaxing solution for 2 minutes. (5) The samples were sealed and air dried. (6) Microscopic examination.

Statistical analysis

Image-Pro Plus software was used to convert the immunohistochemistry patterns into aver-

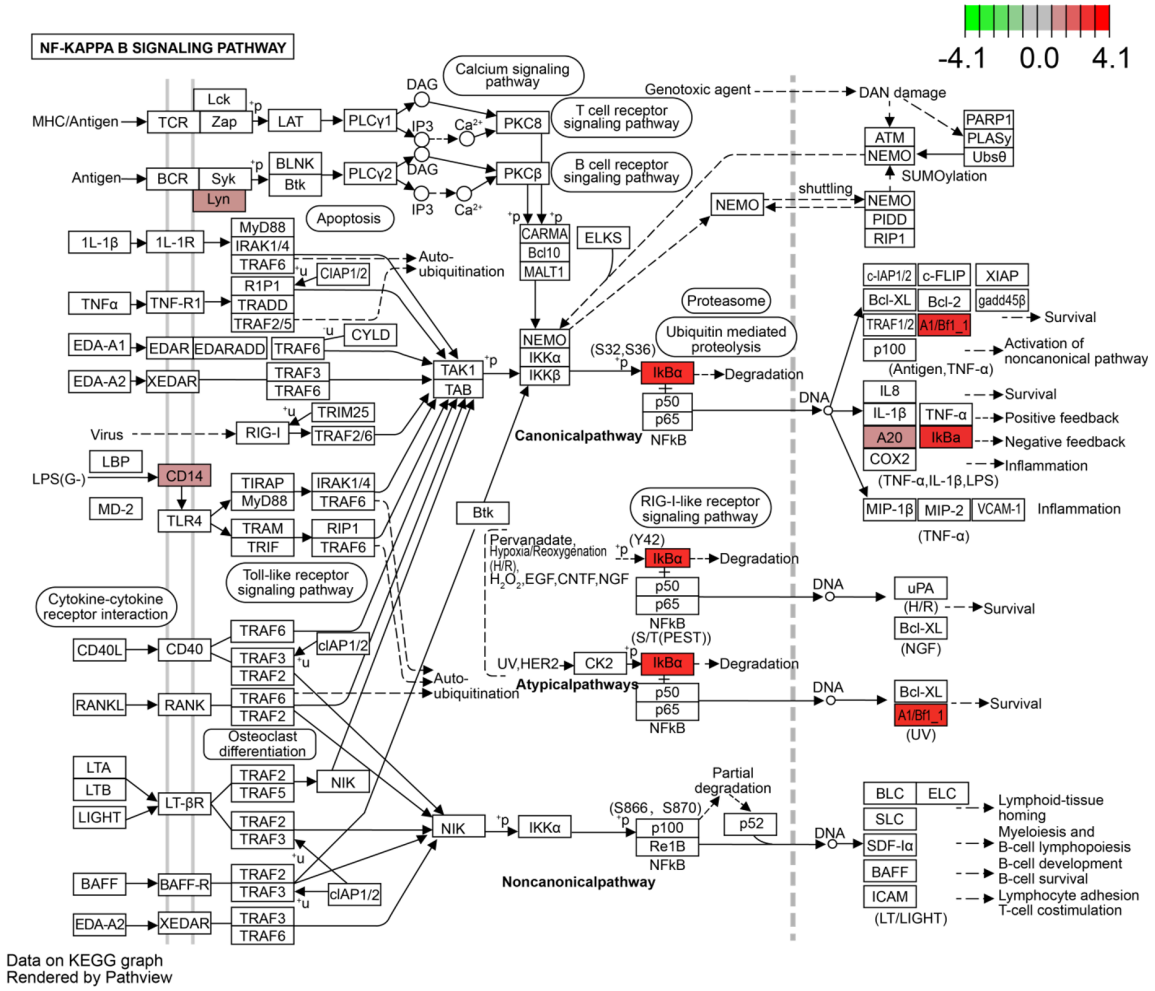

Figure 8. NF-κB signalling pathway in the KD-CALs group. KD: Kawasaki disease; CALs: coronary artery lesions.

age optical density values for quantitative analysis. Data were presented as the mean ± standard deviation ($x \pm SD$) or median (range: minimum, maximum) from at least three independent experiments. One-way analysis of variance (one-way ANOVA) with the Newman-Keuls comparison test was employed to determine significant differences between groups. Statistical analysis was carried out using SPSS 17.0 software. A level of $P < 0.05$ was considered statistically significant.

Results

Clinical information

Comparison of clinical information: There were no significant differences in the general information except age and weight between the two groups (**Table 5**). The clinical manifestations did not significantly differ between the two groups (**Table 6**).

Differentially expressed genes in the acute and subacute stages in the CALs and nCALs groups: mRNA microarray revealed that both the CALs group and the nCALs group had numerous highly expressed genes among the PBMC samples. As shown in **Figure 2A**, **2C**, there were 60 DEGs between the acute and subacute stages in the KD-nCALs group, 42 of which were upregulated and 18 of which were downregulated ($P < 0.05$). In the two stages of the KD-CALs group (**Figure 2B**, **2D**), 62 genes presented different expression patterns, 50 of which were upregulated and 12 of which were downregulated ($P < 0.05$).

Gene set enrichment analysis: GO analysis revealed that the DEGs in KD-nCALs were

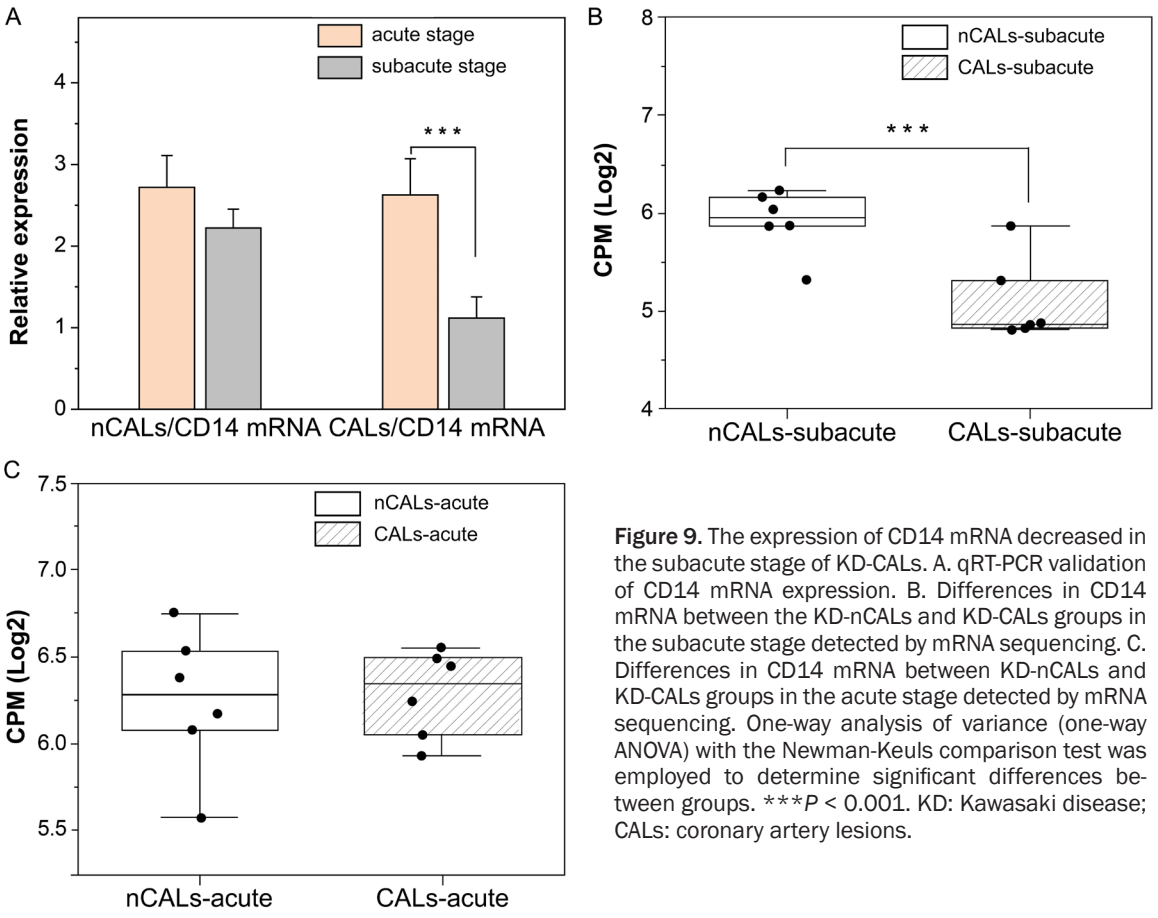

Figure 9. The expression of CD14 mRNA decreased in the subacute stage of KD-CALs. A. qRT-PCR validation of CD14 mRNA expression. B. Differences in CD14 mRNA between the KD-nCALs and KD-CALs groups in the subacute stage detected by mRNA sequencing. C. Differences in CD14 mRNA between KD-nCALs and KD-CALs groups in the acute stage detected by mRNA sequencing. One-way analysis of variance (one-way ANOVA) with the Newman-Keuls comparison test was employed to determine significant differences between groups. ***$P < 0.001$. KD: Kawasaki disease; CALs: coronary artery lesions.

enriched in negative regulation of haemopoiesis, nuclear-transcribed mRNA catabolic process, and pattern recognition receptor signalling pathway (**Figure 3**). Moreover, neutrophil-mediated immunity, immune response-related neutrophil degranulation, neutrophil activation, and leukocyte degranulation - all related to inflammation - were enriched primarily in KD-CALs (**Figure 4**). KEGG pathway enrichment analysis identified the top 30 pathways to better understand the important functions of the differentially expressed mRNAs. We found that the screened differential genes of KD-nCALs were enriched mainly in the ribosome and chemokine signalling pathways (**Figure 5**). Moreover, the DEGs of KD-CALs were significantly enriched in the NF-κB signalling pathway (**Figure 6**).

The details of NF-κB signalling pathway are displayed in **Figures 7**, **8**. Surprisingly, we detected a differential gene encoding CD14 mRNA. As shown in **Figure 8**, the expression of CD14 mRNA was significantly upregulated in the NF-κB signalling pathway in the KD-CALs group. However, this enrichment was not observed in the KD-nCALs groups (**Figure 7**). The outcome aligned with the information obtained from the heatmap.

Expression levels of CD14 mRNAs and downstream genes in patients with KD: According to the RNA sequencing data, the expression levels of CD14 mRNA were elevated in the acute stage compared with the subacute stage of KD-CALs, but there was no difference between these two stages of KD-nCALs. Furthermore, qRT-PCR was used to validate the change in CD14-mRNA expression in patients with KD (6 new cases of nCALs in the two stages and 6 new cases of CALs in the two stages). In KD-CALs, CD14-mRNA expression was dramatically lower, by approximately 2-fold, in the subacute stage ($P < 0.001$) compared with the acute stage (**Figure 9A**), and there was no discernible change between the two stages in the KD-nCALs, which was consistent with the RNA-seq results. In addition, the expression of CD14

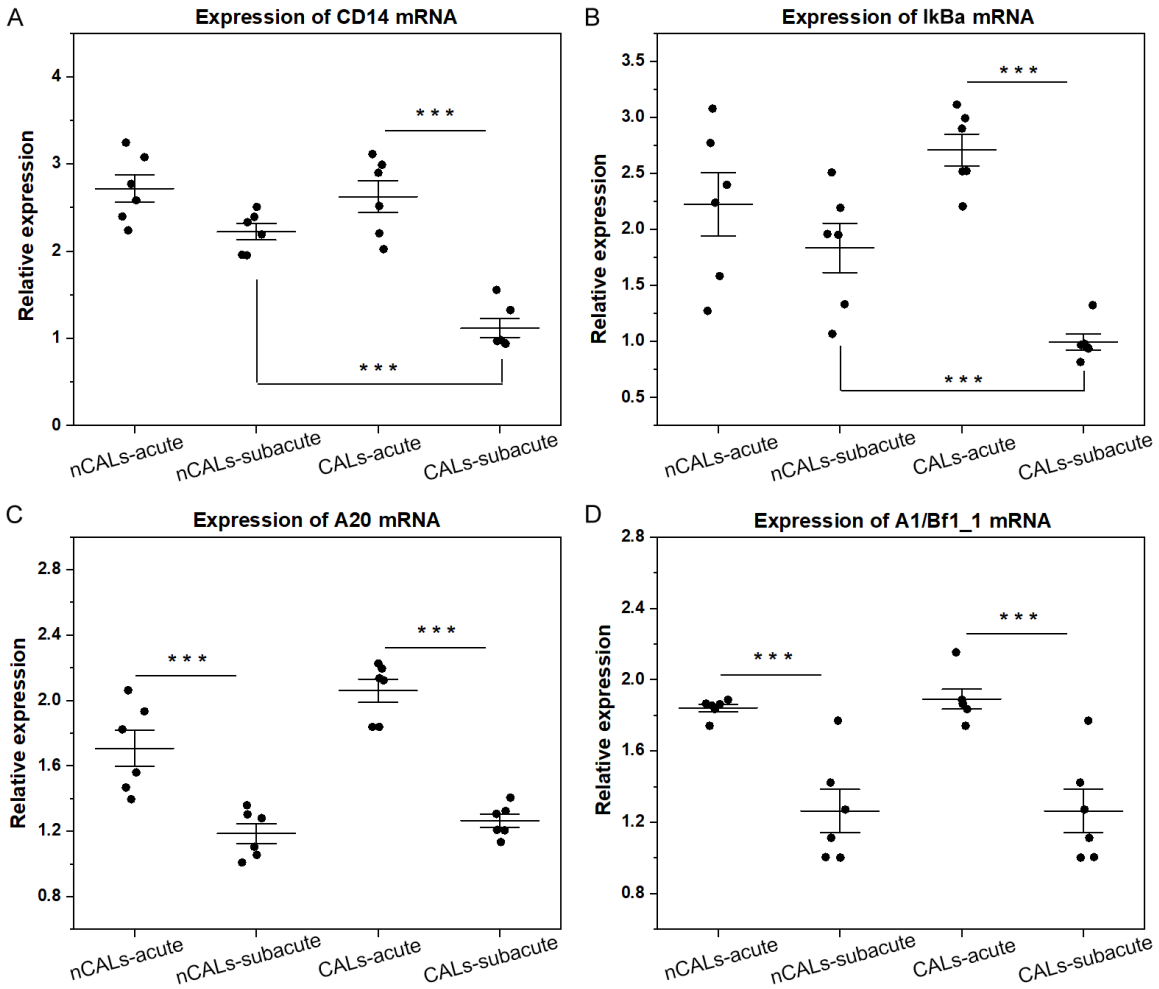

Figure 10. Expression of CD14 mRNA and downstream genes in the KD groups. (A-D) Indicate the relative expression of CD14, IκBα, A20, and A1/Bf1_1 in the nCALs-acute, nCALs-subacute, CALs-acute, and CALs-subacute groups of KD, respectively. One-way ANOVA with the Newman-Keuls comparison test was employed to determine significant differences between groups. ***$P < 0.001$. KD: Kawasaki disease; CALs: coronary artery lesions.

mRNA in CALs was lower than that in nCALs in the subacute stage of KD (**Figure 9B**), but there was no significant difference in the acute stage between the two groups (**Figure 9C**).

On the basis of KEGG analysis, the upregulation of CD14 mRNA might affect the expression of downstream genes. Additionally, the expression of IκBα, A20, and A1/Bf1_1 was investigated via qRT-PCR. In KD-CALs, the expression of IκBα was lower in the subacute stage compared with the acute stage, but this change was not observed in KD-nCALs (**Figure 10B**). In the comparison between groups, the expression of IκBα in KD-CALs was lower than that in KD-nCALs in the subacute stage, and there were no differences in the acute stage between the two groups (**Figure 10A**, **10B**). In both KD-nCALs and KD-CALs, the expression of A20 and A1/BF1_1 was greater in the acute stage than in the subacute stage (**Figure 10C**, **10D**), which was consistent with the KEGG results. Furthermore, the STRING online tool was used to explore protein networks, and we obtained the top 50 key proteins related to CD14. Hub genes, such as TLR4, TNF receptor-associated factor 6 (TRAF6), and MYD88, are downstream genes of CD14 in the NF-κB signalling pathway (**Figure 11**).

Molecular docking: Approximately 3000 small molecules were selected from the TCM database in Taiwan. The binding energy was used to evaluate the binding power between small mol-

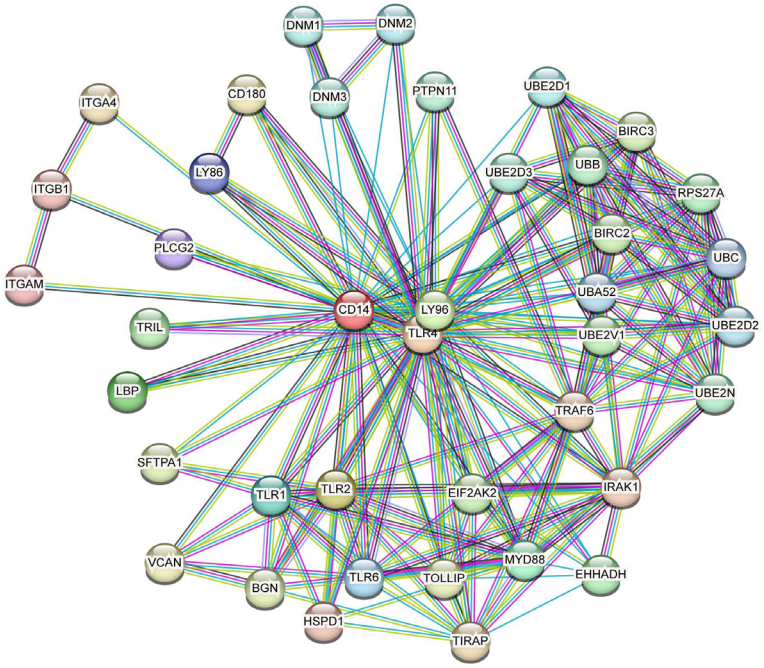

Figure 11. The expression of CD14-related proteins was determined via the STRING tool.

ecules and mCD14. A binding energy < 0 indicated that the molecules could bind spontaneously to the protein. A binding energy < -5 kcal/mol showed a strong binding, and a lower binding energy reflected stronger binding. **Figure 12** shows the binding mode of mCD14 with 5 small molecules, including lupenone (**Figure 12A**), menisine (**Figure 12B**), 3hydroxytirucallic acid (**Figure 12C**), rheindiglucoside (**Figure 12D**), and clematichinenosideAR7 (**Figure 12E**). As shown in **Table 7**, lupenone was the component with the lowest binding energy (-9.9 kcal/mol). Taking **Figure 12E** as an example, clematichinenosideAR7 underwent hydrogen binding with several amino acid residues of mCD14 after entering the active site.

Animal experiments

Pathological section: On Day 7, there was no significant inflammation of the coronary endothelium in the model mice (**Figure 13C**, **13D**), but on Day 14, significant endothelial inflammation was observed (**Figure 13E**, **13F**). Pathology revealed significant infiltration of lymphocytes and macrophages into the coronary artery endothelium of the mice on Day 14, whereas the endothelial structure of the control group mice was normal (**Figure 13A**, **13B**).

Changes in the mCD14, IκBα and IL-6 proteins in the mouse coronary artery endothelium: Immunohistochemistry revealed that the mCD14, IκBα and IL-6 protein levels in the coronary endothelium significantly increased in the Day 14 group (**Figures 14**-**16**). Quantitative analysis showed that the mCD14, IκBα and IL-6 protein levels in the coronary endothelium significantly increased in the Day 14 group, compared with those in the other two groups ($P < 0.05$) (**Figure 17**).

Discussion

Since KD can result in permanent, severe coronary artery lesions, thus, investigations to identify biomarkers and the underlying mechanism have continued [23]. Some studies have focused on determining the gene expression characteristics of KD through database analysis. Nie et al. used the Gene Expression Omnibus Database to obtain databases related to KD (GSE18606, GSE68004, and GSE73641), and the data were integrated with samples from patients with KD and normal controls [24]. By analysing the expression profiles of samples from patients with KD and healthy controls, Hu et al. identified 332 crucial genes associated with KD [25]. There has been no research on potential molecular markers of coronary artery injury in KD.

In our research, we categorized patients with KD in greater detail to search for molecular mechanisms and potential molecular markers of coronary artery lesions. We divided patients with KD into CALs and nCALs according to the *Z* value, and each group was subdivided into acute and subacute stages based on their specific onset of disease. The general information and clinical manifestations of patients in the CALs and nCALs groups were first compared. We found that the age of patients in the CALs group was lower than that of patients in the nCALs group, which is consistent with previous reports that low age is a risk factor for KD-CALs

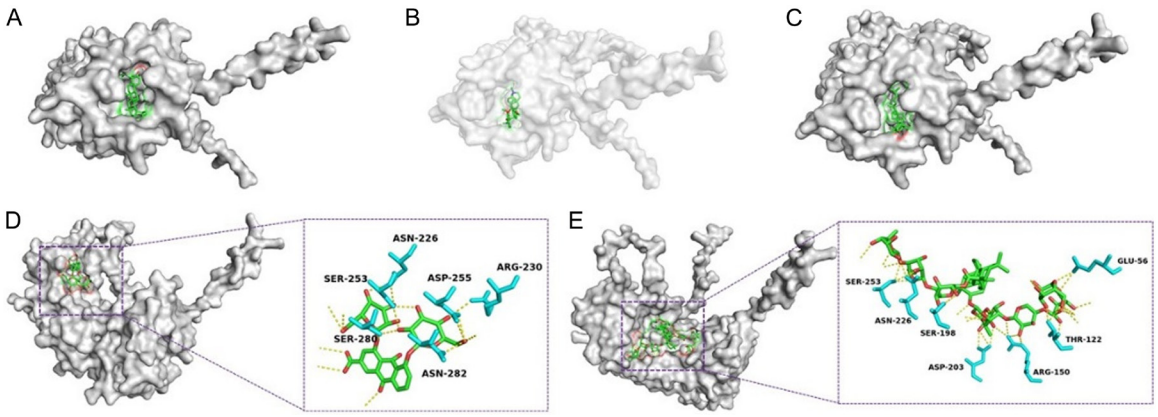

Figure 12. Docking results of 5 groups of molecules with optimal binding energies. A. Molecular binding diagram of lupenone with mCD14. B. Molecular binding diagram of Menisine with mCD14. C. Molecular binding diagram of 3-hydroxytirucallic acid with mCD14. D. Molecular binding diagram of rheindiglucoside with mCD14. E. Molecular binding diagram of clematichinenosideAR7 with mCD14.

Table 7. The binding energy data for all 5 molecules

Molecule	Binding energy with mCD14	Corresponding traditional Chinese medicine
Lupenone	-9.9 kcal/mol	Hedysarum Multijugum Maxim
Menisine	-9.9 kcal/mol	
3hydroxytirucallicacid	-9.8 kcal/mol	Olibanun
Rheindiglucoside	-9.8 kcal/mol	Radix Rhei Et Rhizome Sennae Folium Polygoni Cuspidati Rhizoma Et Radix
ClematichinenosideAR7	-9.7 kcal/mol	Smilax Scobinicaulis C.H. Wright

[26]. Considering the correlation between weight and age, there was also a significant difference in weight between the two groups. In addition, there was no significant difference in sex, clinical manifestations, or response to immunoglobulin between the two groups, which suggested that patients with KD-CALs often do not exhibit specific clinical symptoms.

Through DEG analysis, we identified 60 DEGs between the two stages in the nCALs group and 62 DEGs in the CALs group. The DEGs of KD-nCALs were enriched mainly in the ribosome and chemokine signalling pathways, whereas high enrichment of the NF-κB signalling network was observed in the DEGs of KD-CALs. Moreover, CD14 mRNA was highly expressed in the NF-κB signalling pathway, but this phenomenon did not occur in KD-nCALs. Combined with the RNA-seq and qRT-PCR validation results, we found that in the KD-CALs group, the expression of CD14 mRNA was significantly upregulated in the acute stage compared with the subacute stage. However, in the nCALs group, there was no difference in the expression of CD14 mRNA between the two stages. Previous studies have shown that the transcription and protein expression of CD14 in monocytes in atherosclerotic lesions are significantly increased [27], and many vascular diseases also involve NF-κB activation [12]. Therefore, based on those clinical trial results, we speculated that CD14 mRNA and the NF-κB signalling pathway were involved in the inflammatory process of KD-CALs.

IκBα is one of the most important members of the inhibitory protein family that regulates NF-κB [28]. In our study, we found that IκBα, a downstream gene of CD14 mRNA in the NF-κB pathway, was upregulated in KD-CALs but not in KD-nCALs. Although the precise connection between the CD14 and IκBα genes was not clear, in the KEGG analysis and qRT-PCR validation, changes in the expression of the CD14 and IκBα genes were synchronous between the two groups. The other downstream genes, A20 and A1/Bf1_1, were upregulated in both

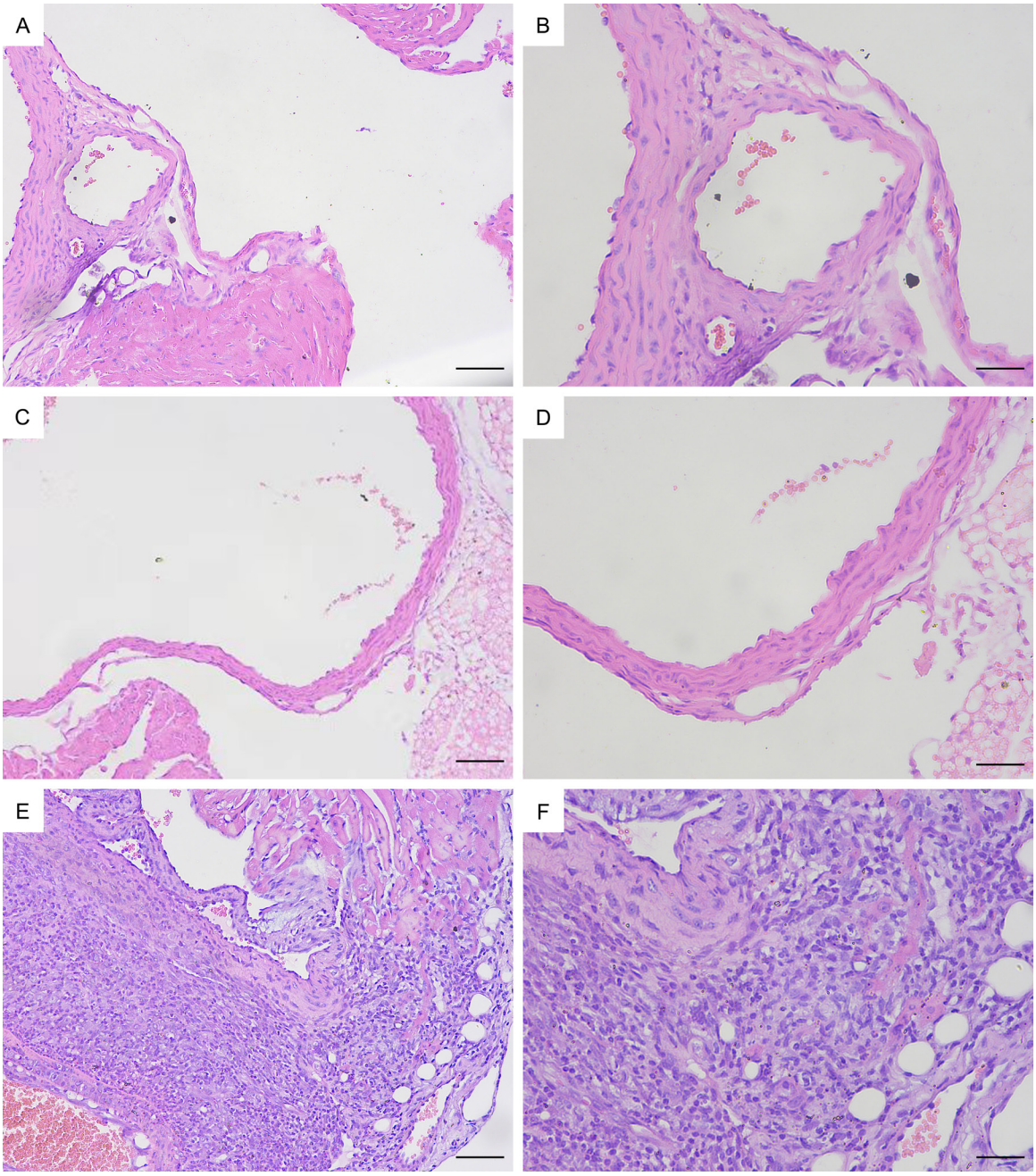

Figure 13. H&E staining of pathological sections of the mouse coronary endothelium. (A) Control group ×200. (B) Control group ×400. (C) Day 7 group of modelling ×200. (D) Day 7 group of modelling ×400. (E) Day 14 group of modelling ×200. (F) Day 14 group of modelling ×400. Bar = 100 μm (A, C, E), 50 μm (B, D, F).

groups, and their expression changes in the two groups were not completely consistent with those of CD14. Transcription of A20 (TNF-α-induced protein 3 or TNFAIP3) can be activated by NF-κB signalling, resulting in negative feedback on NF-κB [29]. Therefore, we hypothesized that the upregulation of CD14 mRNA might increase the expression of IkBα and subsequently activate NF-κB signalling, thus playing a role in coronary inflammation. Conversely, A20 is subsequently activated by NF-κB, and activated A20 has negative feedback effects on the NF-κB signalling pathway. As a balancing mechanism, A20 can inhibit excessive inflammatory responses, which reflects the complexity of the inflammatory network.

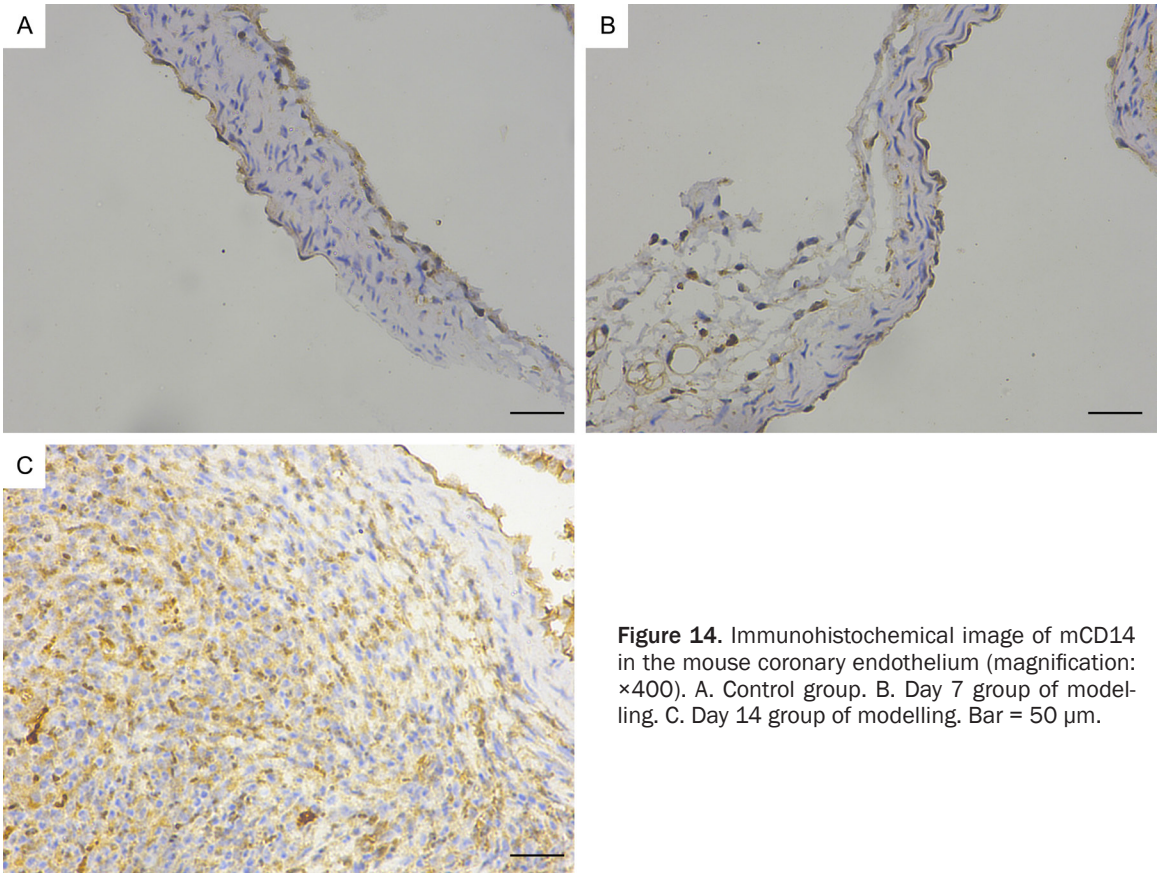

Figure 14. Immunohistochemical image of mCD14 in the mouse coronary endothelium (magnification: ×400). A. Control group. B. Day 7 group of modelling. C. Day 14 group of modelling. Bar = 50 μm.

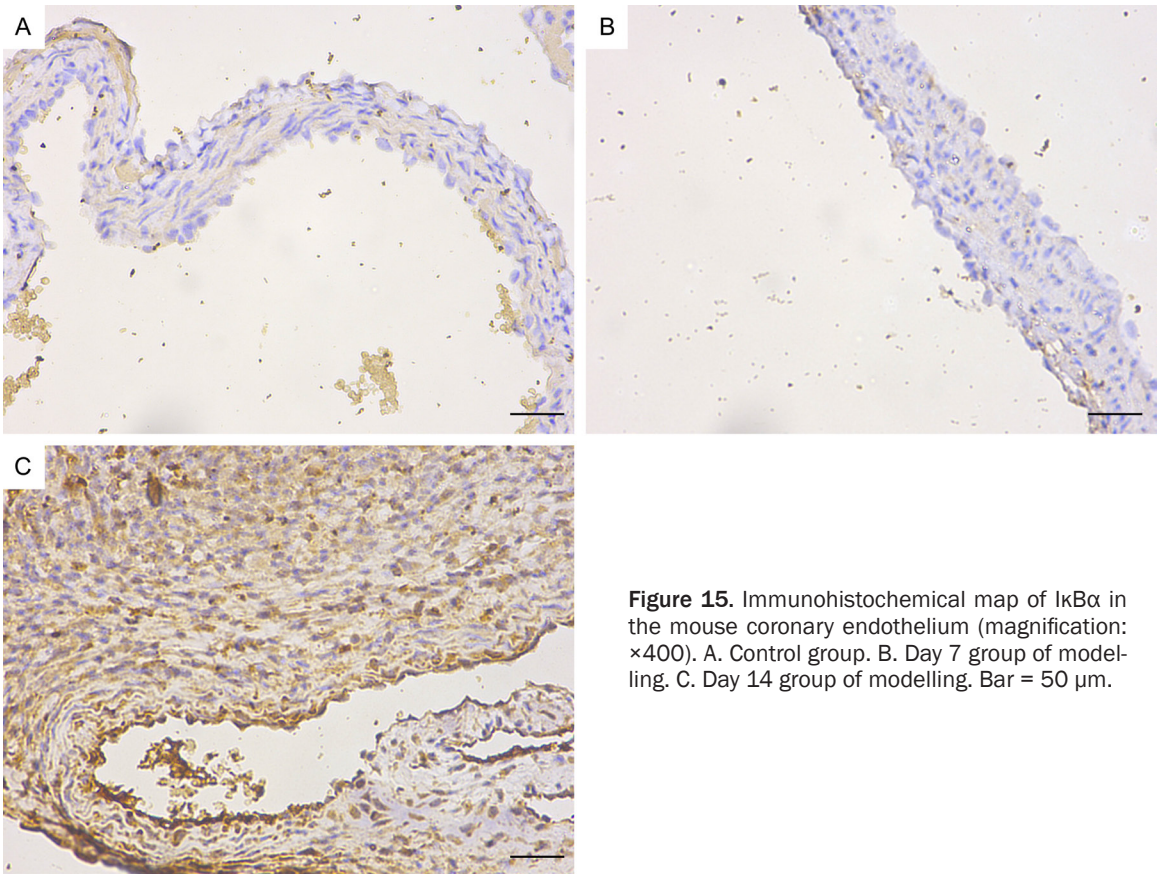

Figure 15. Immunohistochemical map of IκBα in the mouse coronary endothelium (magnification: ×400). A. Control group. B. Day 7 group of modelling. C. Day 14 group of modelling. Bar = 50 μm.

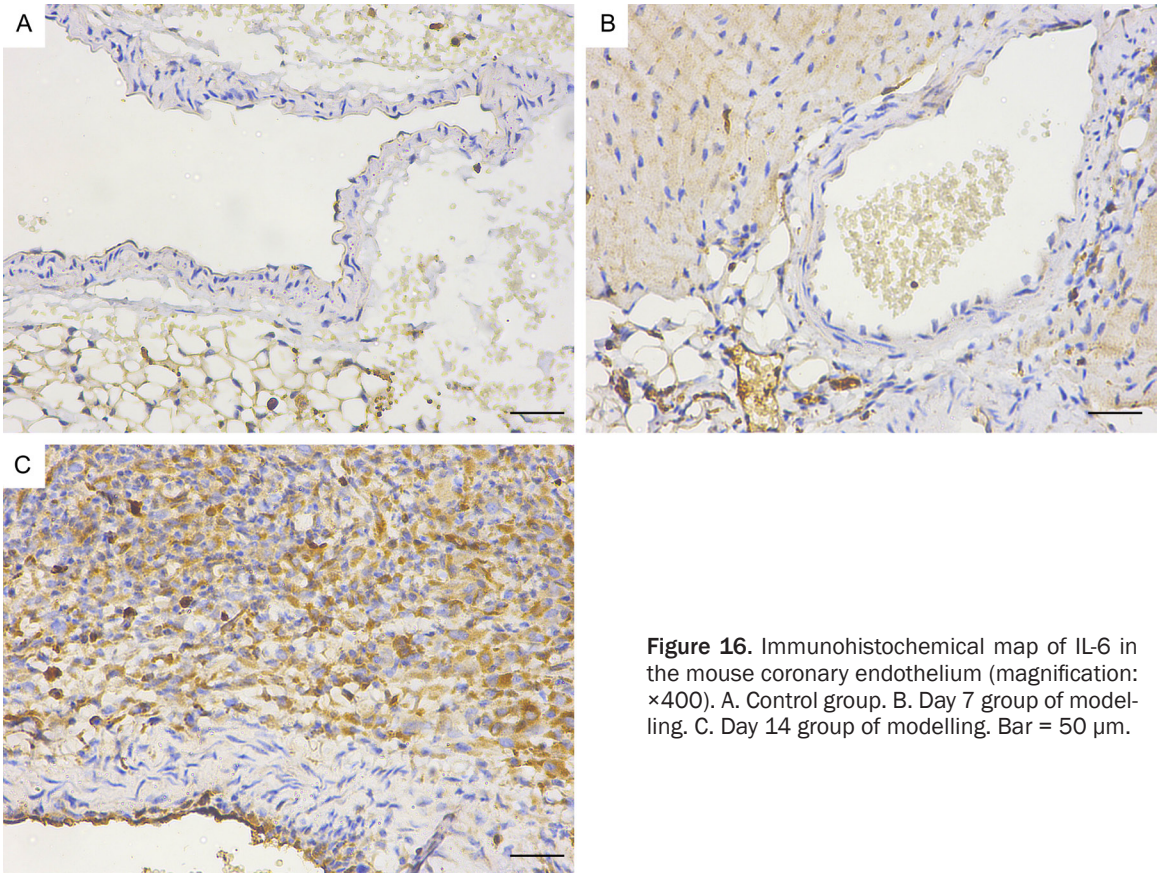

Figure 16. Immunohistochemical map of IL-6 in the mouse coronary endothelium (magnification: ×400). A. Control group. B. Day 7 group of modelling. C. Day 14 group of modelling. Bar = 50 μm.

In addition to gene transcription, we needed to validate the roles of the CD14 and IκBα proteins in KD-CALs. Considering the difficulty of obtaining coronary arteries from patients with KD, we established a KD mouse model to observe changes in coronary arteries and CD14 and IκBα proteins at different stages. IL-6 is a conventional inflammatory marker that can be secreted by monocytes during activation and endothelial cell injury. The level of IL-6 reflects the inflammatory state, so we also measured the level of IL-6 protein in the coronary arteries to determine the degree of inflammation. To observe dynamic changes in coronary inflammation and the corresponding proteins in the mice and to determine whether the model was successful, we established samples at different time points after the model was established. We found that on Day 7 after completion of modelling, inflammation in the coronary artery tissue of the mice was not obvious. On Day 14 after completion of modelling, obvious inflammation appeared in the endothelial cells of the mouse coronary arteries, manifested as infiltration of lymphocytes and macrophages. According to previous studies, beginning on Day 14 after intraperitoneal injection of CAWS, significant immune cell infiltration occurred in the coronary arteries of C57BL/6J mice [30]. Monocytes and macrophages were identified as the main inflammatory cell types infiltrating the KD coronary arteries, which was consistent with our animal experiment results. Therefore, the mouse model of KD-CALs was considered to be successfully established. On Day 14, the protein levels of mCD14, IκBα, and the inflammatory cytokine IL-6 in the coronary endothelium also increased significantly compared with those on Day 7 and in the control group. As the coronary arteries gradually exhibited inflammation, the protein levels of mCD14, IκBα, and the inflammatory cytokine IL-6 also gradually increased in a synchronous manner. The results of the animal experiments confirmed the speculation of our clinical trials. At the protein level, the CD14 and NF-κB signalling pathways were also involved in the inflammatory process of KD-CALs; thus, it could be inferred that CD14 mRNA and its protein mCD14 played important roles in the inflammatory response of KD-CALs.

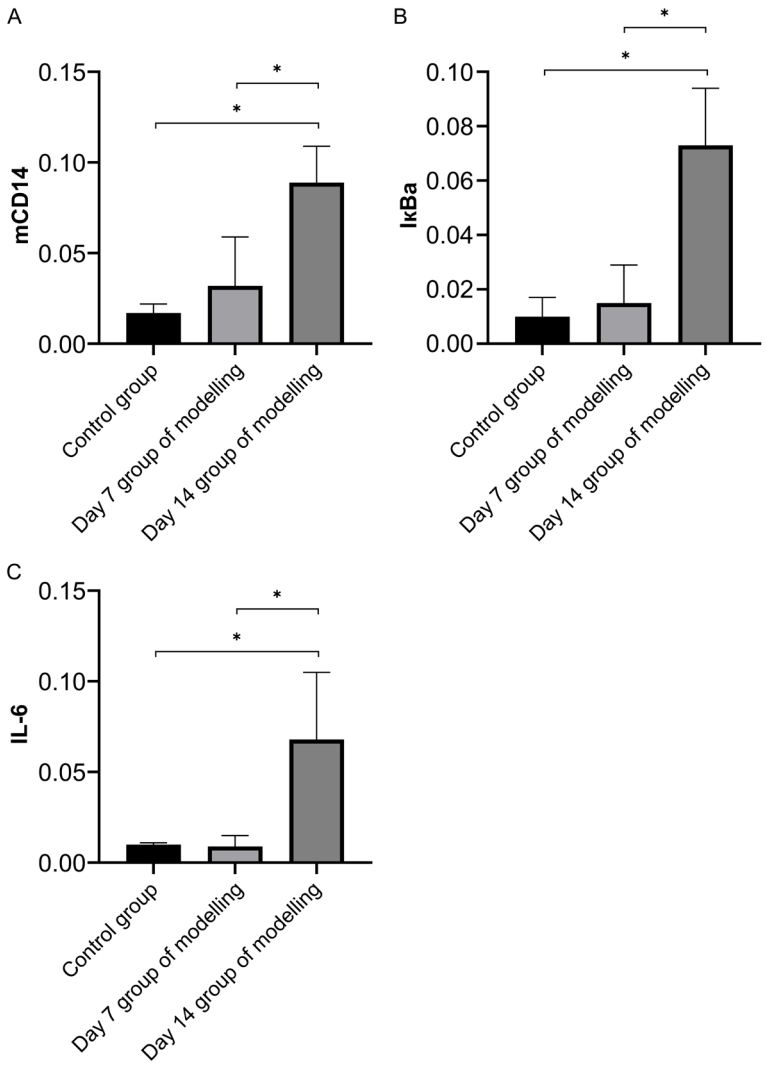

Figure 17. The mCD14 (A), IκBα (B) and IL-6 (C) protein levels in the coronary endothelium significantly increased in the Day 14 group. Image-Pro Plus software was used to convert the immunohistochemistry patterns into average optical density values, and one-way ANOVA with the Newman-Keuls comparison test was employed to determine significant differences between groups. *$P < 0.05$.

KD is characterized by systemic small- and medium-sized arteritis; although early treatment with aspirin and intravenous gamma globulin can reduce the incidence of coronary artery lesions, some children remain insensitive to treatment [31]. Many studies have reported the therapeutic effects and mechanisms of TCM on coronary artery injury in KD [32, 33]. We found that the CD14 gene and protein were involved in the signalling networks of KD-CALs; therefore, we explored whether there might be a connection between the CD14 protein and TCM to search for new methods for treating KD-CALs. Through molecular docking, we screened five small-molecule compounds that could bind strongly with mCD14. Among these compounds, lupenone demonstrated the strongest ability to bind to mCD14. Lupenone, which is isolated from Musa basjoo, is a lupine-type triterpenoid molecule with antiviral and anti-inflammatory properties. As lupenone is an active component of Hedysarum Multijugum Maxim, we predict that Hedysarum Multijugum Maxim may suppress the inflammatory response by targeting mCD14 with lupenone and that mCD14 may become a potential therapeutic target; however, owing to limitations in experimental conditions and time, we have not validated this finding, necessitating further research in the future.

The limitations of our research include the absence of a comprehensive exploration into the mechanism of CD14 mRNA in KD-CALs and the mechanism of CD14 mRNA in regulating IκBα. Consequently, more in depth research is needed in the future.

Conclusions

According to our research, CD14 mRNA may affect IκBα expression and activate the NF-κB signalling pathway, resulting in inflammation of vascular endothelial cells and ultimately leading to coronary artery dilation in patients with KD. We predict that CD14 mRNA can play a significant role in coronary artery injury in KD. Molecular docking suggested that mCD14 may be a therapeutic target for CALs in KD.

Acknowledgements

We thank Bo Wang and Hui-Juan Kan for the sample collection from the patients. We

express our gratitude to the whole team members for their constructive advice. We thank Prof. Chunfu Zheng (University of Calgary, Canada) for language editing. Support is available from the National Natural Science Foundation of China grant: 82000467.

Disclosure of conflict of interest

None.

Address correspondence to: Wenhua Yan, Department of Cardiology, Children's Hospital of Soochow University, No. 92, Zhongnan Street, Suzhou Industrial Park, Suzhou, Jiangsu, China. Tel: +86-13584881508; E-mail: whyan328@sina.com

References

[1] Seki M and Minami T. Kawasaki disease: pathology, risks, and management. Vasc Health Risk Manag 2022; 18: 407-416.
[2] Piram M and Burns JC. Kawasaki disease for the paediatric dermatologist: skin manifestations and new insights into the pathophysiology. Clin Exp Dermatol 2021; 46: 503-509.
[3] Kuo HC. Diagnosis, progress, and treatment update of Kawasaki disease. Int J Mol Sci 2023; 24: 13948.
[4] Huang B, Tan W, Liao S and Jiang W. Clinical characteristics of Kawasaki disease in children with different age groups: a literature review and retrospective study. Curr Pharm Des 2023; 29: 1516-1523.
[5] Madan D, Maheshwari A, Mahto D, Mendiratta V and Sharma S. Kawasaki disease with peripheral and facial gangrene: a case report and review of literature. Trop Doct 2022; 52: 449-452.
[6] Kainth R and Shah P. Kawasaki disease: origins and evolution. Arch Dis Child 2021; 106: 413-414.
[7] Scherler L, Haas NA, Tengler A, Pattathu J, Mandilaras G and Jakob A. Acute phase of Kawasaki disease: a review of national guideline recommendations. Eur J Pediatr 2022; 181: 2563-2573.
[8] Gupta A. Kawasaki disease and infections: a myth or a reality? Indian J Pediatr 2022; 89: 747-748.
[9] Bordea MA, Costache C, Grama A, Florian Al, Lupan I, Samasca G, Deleanu D, Makovicky P, Makovicky P and Rimarova K. Cytokine cascade in Kawasaki disease versus Kawasaki-like syndrome. Physiol Res 2022; 71: 17-27.
[10] Ming L, Cao HL, Li Q and Yu G. Red blood cell distribution width as a predictive marker for coronary artery lesions in patients with Kawasaki disease. Pediatr Cardiol 2021; 42: 1496-1503.
[11] Zinatizadeh MR, Schock B, Chalbatani GM, Zarandi PK, Jalali SA and Miri SR. The nuclear factor kappa B (NF-κB) signaling in cancer development and immune diseases. Genes Dis 2021; 8: 287-297.
[12] Li S, Xu Z, Wang Y, Chen L, Wang X, Zhou Y, Lei D, Zang G and Wang G. Recent advances of mechanosensitive genes in vascular endothelial cells for the formation and treatment of atherosclerosis. Genes Dis 2023; 11: 101046.
[13] Khan D, Cornelius JF and Muhammad S. The role of NF-κB in intracranial aneurysm pathogenesis: a systematic review. Int J Mol Sci 2023; 24: 14218.
[14] Sharygin D, Koniaris LG, Wells C, Zimmers TA and Hamidi T. Role of CD14 in human disease. Immunology 2023; 169: 260-270.
[15] Na K, Oh BC and Jung Y. Multifaceted role of CD14 in innate immunity and tissue homeostasis. Cytokine Growth Factor Rev 2023; 74: 100-107.
[16] Geng Z, Tao Y, Zheng F, Wu L, Wang Y, Wang Y, Sun Y, Fu S, Wang W, Xie C, Zhang Y and Gong F. Altered monocyte subsets in Kawasaki disease revealed by single-cell RNA-sequencing. J Inflamm Res 2021; 14: 885-896.
[17] Liu X, Luo T, Fan Z, Li J, Zhang Y, Lu G, Lv M, Lin S, Cai Z, Zhang J, Zhou K, Guo J, Hua Y, Zhang Y and Li Y. Single cell RNA-seq resolution revealed CCR1+/SELL+/XAF+ CD14 monocytes mediated vascular endothelial cell injuries in Kawasaki disease and COVID-19. Biochim Biophys Acta Mol Basis Dis 2023; 1869: 166707.
[18] Aguilar Briseño JA, Ramos Pereira L, van der Laan M, Pauzuolis M, Ter Ellen BM, Upasani V, Moser J, de Souza Ferreira LC, Smit JM and Rodenhuis-Zybert IA. TLR2 axis on peripheral blood mononuclear cells regulates inflammatory responses to non-infectious immature dengue virus particles. PLoS Pathog 2022; 18: e1010499.
[19] Yang HY, Liu ML, Luo P, Yao XS and Zhou H. Network pharmacology provides a systematic approach to understanding the treatment of ischemic heart diseases with traditional Chinese medicine. Phytomedicine 2022; 104: 154268.
[20] Wang Y, Su Y, Lai W, Huang X, Chu K, Brown J and Hong G. Salidroside restores an anti-inflammatory endothelial phenotype by selectively inhibiting endothelial complement after oxidative stress. Inflammation 2020; 43: 310-325.
[21] Tang B, Lo HH, Lei C, U KI, Hsiao WW, Guo X, Bai J, Wong VK and Law BY. Adjuvant herbal therapy for targeting susceptibility genes to Kawasaki disease: an overview of epidemiology,

pathogenesis, diagnosis and pharmacological treatment of Kawasaki disease. Phytomedicine 2020; 70: 153208.

[22] McCrindle BW, Rowley AH, Newburger JW, Burns JC, Bolger AF, Gewitz M, Baker AL, Jackson MA, Takahashi M, Shah PB, Kobayashi T, Wu MH, Saji TT and Pahl E; American Heart Association Rheumatic Fever, Endocarditis, and Kawasaki Disease Committee of the Council on Cardiovascular Disease in the Young; Council on Cardiovascular and Stroke Nursing; Council on Cardiovascular Surgery and Anesthesia; and Council on Epidemiology and Prevention. Diagnosis, treatment, and long-term management of Kawasaki disease: a scientific statement for health professionals from the American Heart Association. Circulation 2017; 135: e927-e999.

[23] Xiong Y, Xu J, Zhang D, Wu S, Li Z, Zhang J, Xia Z, Xia P, Xia C, Tang X, Liu X, Liu J and Yu P. MicroRNAs in Kawasaki disease: an update on diagnosis, therapy and monitoring. Front Immunol 2022; 13: 1016575.

[24] Nie H, Wang S, Wu Q, Xue D and Zhou W. Five immune-gene-signatures participate in the development and pathogenesis of Kawasaki disease. Immun Inflamm Dis 2021; 9: 157-166.

[25] Hu B, Li Y, Wang G and Zhang Y. The blood gene expression signature for Kawasaki disease in children identified with advanced feature selection methods. Biomed Res Int 2020; 2020: 6062436.

[26] Wang L, Zeng X and Chen B. Clinical manifestations and risk factors of coronary artery lesions in children with Kawasaki disease. Medicine (Baltimore) 2023; 102: e34939.

[27] Kim BY, Son Y, Kim BJ, Chung SW, Lee D, Eo SK and Kim K. Atheroma-relevant 7-oxysterols differentially upregulate Cd14 expression. Int J Mol Sci 2023; 24: 10542.

[28] Sang R, Sun F, Zhou H, Wang M, Li H, Li C, Sun X, Zhao X and Zhang X. Immunomodulatory effects of Inonotus obliquus polysaccharide on splenic lymphocytes infected with Toxoplasma gondii via NF-κB and MAPKs pathways. Immunopharmacol Immunotoxicol 2022; 44: 129-138.

[29] Mooney EC and Sahingur SE. The ubiquitin system and A20: implications in health and disease. J Dent Res 2021; 100: 10-20.

[30] Noval Rivas M and Arditi M. Kawasaki disease: pathophysiology and insights from mouse models. Nat Rev Rheumatol 2020; 16: 391-405.

[31] Sapountzi E, Fidani L, Giannopoulos A and Galli-Tsinopoulou A. Association of genetic polymorphisms in Kawasaki disease with the response to intravenous immunoglobulin therapy. Pediatr Cardiol 2023; 44: 1-12.

[32] Yang Y, Wang N, Wang Z, Zhao M, Chen L and Shi Z. Protective role of forsythoside B in Kawasaki disease-induced cardiac injury: inhibition of pyroptosis via the SIRT1-NF-κB-p65 signaling pathway. Chem Biol Interact 2024; 392: 110953.

[33] Zhang J, Zhuge Y, Rong X, Ni C, Niu C, Wen Z, Lin H, Chu M and Jia C. Protective roles of Xijiao Dihuang Tang on coronary artery injury in Kawasaki disease. Cardiovasc Drugs Ther 2023; 37: 257-270.